Voltage Sag Data Utilization for Distribution Fault Location

Saeed Lotfifard, *Student Member, IEEE*, Mladen Kezunovic, *Fellow, IEEE*, and Mirrasoul J. Mousavi, *Member, IEEE*

Abstract—Fault location in distribution systems is an important function for outage management and service restoration directly impacting feeder reliability. In this paper, a fault location method based on matching calculated voltage sag data and data gathered at some nodes in the network is proposed. A method for characterization of voltage sags is utilized to reduce amount of transferred data. The proposed method can pinpoint fault location precisely, and is applicable to any complex distribution systems with load taps, laterals, and sub-laterals, single-phase loads, as well as networks with heterogeneous lines. The performance of the proposed method is demonstrated on the IEEE 123-node distribution test system via computer simulations in Alternate Transients Program software.

Index Terms—Distribution system, fault location, voltage sag characteristic.

I. INTRODUCTION

FOLLOWING the detection of a sustained fault in distribution systems, its location must be determined for service restoration and damage repair. Unlike protective relaying that is an online application requiring real-time operation, fault location is typically an offline application for which the accuracy is the main objective [1]. Yet, it is also true that the faster the fault location is determined, the sooner the faulted area is identified and isolated from the healthy parts of the feeder. As a result, the service reliability and customer satisfaction indices will be improved.

To date, a number of methods have been proposed for fault location on transmission lines but they are not easily applicable to distribution systems. This is mainly due to the existence of short and heterogeneous lines, presence of laterals, load taps, and comparatively a lower degree of instrumentation in distribution systems. Therefore, a number of fault location methods have been proposed in the past specifically for distribution systems.

In [2]–[4], the apparent impedance, defined as the ratio of selected voltage to selected current based on the fault type and faulted phases, is utilized for locating faults on distribution systems. Heterogeneity of the lines is not considered in [2]. [3] neglects the dynamic nature of the loads, and the presence of laterals has not been addressed in [4]. A detailed review of this category of methods has been provided in [5]. The common

drawback is that the fault location results in multiple estimations due to their reliance solely on measured voltage and current signals at the substation. In [6], data collected from fault indicators along the network, which determine the direction of the fault, are utilized to solve the multiple fault location estimation problem. Installation of fault indicators at the beginning of each tap increases the implementation cost and may not be a preferred solution.

In [7] and [8], a method based on direct circuit analysis, was suggested. Although it is suitable for unbalanced distribution systems, it does not yield unique results for fault location.

In [9] and [10], a method using superimposed components of the voltages and currents is proposed. In this method, an assumed fault point is varied systematically until the actual fault point is found. The fault is located based on the fact that the amount of the superimposed current in healthy lines should be minimum. This method also suffers from multiple fault location estimations.

Methods based on intelligent systems such as neural networks and fuzzy logics as powerful tools for classification purposes are proposed in [11], [12]. In [11], the faulted area is detected by training an adaptive neuro-fuzzy inference system (ANFIS) net with extracted features based on knowledge about protective device settings. In [12] using the learning algorithm for multivariable data analysis (LAMDA) classification technique, multiple fault location estimation problem is obviated. This method requires a large number of training data and a re-training process subsequent to a change in power system structure.

In [13]–[15], methods based on traveling waves generated by the fault have been suggested. The time difference between successive captured traveling waves data is used for locating the fault. These methods need high frequency sampling which depends on the tower configuration (propagation velocity) and desired accuracy. This high frequency sampling requirement increases implementation cost. Presence of laterals and load taps that reflect traveling waves, which may be confused with those created by the fault, is another difficulty related to application of these methods on distribution systems. These methods may be more applicable to transmission lines where lines are longer, and equipped with better monitoring devices [16].

The fact that fault causes voltage sags with different characteristics at different nodes has been utilized for fault location in [17], [18]. Only the amplitude of the voltage sag has been used which makes the fault location method susceptible to inaccuracies. The method can identify the faulted node but it cannot pinpoint the fault.

In this paper, a fault location approach for distribution systems is proposed based on gathered data from meters installed at some points along the feeder. These meters should be able

to capture voltage phasors such as power quality meters. A mobile telephone network or some other smart grid communication architecture may be used to transmit the recorded data to the control center. The method can pinpoint the fault quickly and precisely and does not suffer from multiple fault location estimation imprecision.

Pre-fault and during-fault voltage and current phasors at the root node (substation), as well as knowledge about faulted phase(s) and fault type are utilized. Pre-fault measurements are used for estimating load variations and updating load models. During-fault data is used for finding the location of the fault. Voltage sags are also gathered from meters installed at some selected nodes along the feeder.

Fault at each node (one at a time) in the modeled network is applied and voltage sags are calculated using a load flow program. The fault location is determined by comparing how well each calculated case matches up to what was actually observed by the meters in the network. The case that shows the highest similarity is considered the location of the fault.

In implementing the proposed method, several issues should be addressed, which are discussed in Sections II–VI.

The performance of the proposed method is demonstrated using the 123-node IEEE test system simulated in the Alternate Transients Program (ATP) environment.

II. VOLTAGE SAG CHARACTERIZATION

Faults at different locations on the feeder produce voltage sags with different magnitudes. However, in some cases, they may produce voltage sags with the same magnitude.

Fig. 1 shows a simple model of a faulted network. Z_s is the source impedance seen at the meter location, Z is the impedance between meter location and the fault, and R_f is the fault resistance. Voltage sag is captured at the meter location. Two cases are assumed for further analysis. A fault occurs at a location where

$$Z = Z_1$$
$$R_f = R_{f1}. \tag{1}$$

And in another case, the fault is characterized with

$$Z = Z_2$$
$$R_f = R_{f2}. \tag{2}$$

In (2), $Z_2 > Z_1$ implies that fault 2 is farther from the meter location. According to Fig. 1, voltage phasors captured by the meter are

$$V_{meter(1)} = \frac{E(Z_1 + R_{f1})}{(Z_s + Z_1 + R_{f1})} \tag{3}$$

$$V_{meter(2)} = \frac{E(Z_2 + R_{f2})}{(Z_s + Z_2 + R_{f2})}. \tag{4}$$

Some values of Rf1 and Rf2 may exist so that

$$|V_{meter(1)}| = |V_{meter(2)}|. \tag{5}$$

In fact, if R_{f2} is smaller than R_{f1} such that voltage drop on R_{f2} and Z_2 equals to that of R_{f1} and Z_1, magnitude of $V_{meter(1)}$ will be equal to $V_{meter(2)}$. While voltage amplitudes
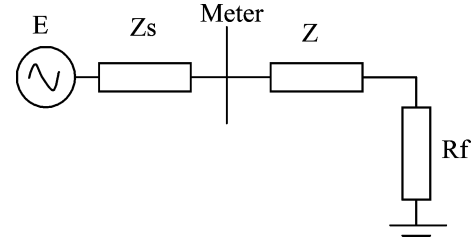

Fig. 1. Simple faulted network model.

can be equal, the phase angles are not the same. As the fault is mainly affected by the resistive part, it produces different angle shift in comparison with line impedance. This difference occurs because the line impedance also has an inductive part that is usually bigger or equal to the resistive part.

Using phase angle shifts in addition to voltage sag magnitudes doubles the volume of the required data. For instance, in case of a single-phase fault in addition to transmitting voltage sag magnitude to the distribution control center, phase angle shift of the faulted phase should be transmitted as well. In the case of three-phase faults, the phase angle shifts for all three phases are required. Therefore, a method should be used to reduce the volume of the required data while preserving the required information.

In [19] a method for three-phase voltage sag characterization has been suggested. A brief description of the method is as follows.

1) The sag type is determined. In [19] each type has been explained in detail. The basic distinction is between types A, C and D. Type A is an equal drop in three phases, type C is a drop in two phases, and type D is a large drop in one phase with a small drop in the other two phases.

   For types C and D, a further subdivision is needed to include the symmetrical phase (the phase with the large voltage drop for type D, the phase without voltage drop for type C). The resulting six types of three-phase unbalanced sags are shown in Fig. 2 [20]. Type D_a is a drop in phase a, type C_a is a drop in phases b and c and so on. Voltage dip type is determined using the phase angle obtained from measurements

   $$T = \frac{1}{60°} \times \arctan\left\{\frac{V_{neq}}{1 - V_{pos}}\right\} \tag{6}$$

   where T is rounded to the nearest integer number and V_{pos} and V_{neg} are the positive and negative sequence voltages, respectively. T can be a number from 0 to 5 that implies the type Ca, Dc, Cb, Da, Cc, and Db, respectively.

2) The characteristic voltage $(\overline{V})$ is calculated which is a phasor that quantifies the severity of the voltage sag. It is defined as

   $$\overline{V} = \overline{V_{pos}} - \overline{V'_{neg}} \tag{7}$$

   where

   $$\overline{V'_{neg}} = \overline{V_{neg}} e^{-jT60°}. \tag{8}$$

3) The positive and negative factor $(\overline{F})$ is an additional phasor to quantify a three-phase unbalanced sag where the
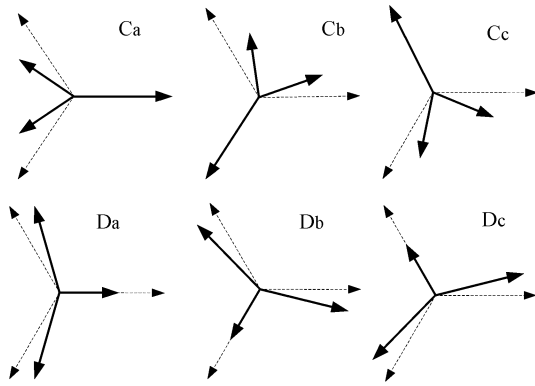
Fig. 2. Types C and D voltage sags for different phases.

Fig. 3. Rf estimation procedure.

system's positive and negative sequence impedances are not equal. It is defined as

$$\overline{F} = \overline{V_{pos}} + \overline{V'_{neg}}. \tag{9}$$

If the negative and positive sequence impedances are equal, $\overline{F}$ is close to unity in all cases. The phasor diagrams in Fig. 2 are given for $\overline{V} = 0.5$ and $\overline{F} = 1$.

The absolute value and the argument of the characteristic voltage $\overline{V}$ are referred to as "magnitude" and "phase-angle jump" of the voltage dip, respectively.

Knowing $\overline{F}$ and $\overline{V}$, it is possible to rebuild the three-phase value of the voltage sag. However, in the proposed fault location method the decision is made based on the comparison of recorded and calculated voltage sag data. This comparison can be done based on $\overline{V}$ which has enough information about amplitude and phase angle jump of the voltage sag. So $\overline{V}$ is the only required data that should be transferred to the distribution control center.
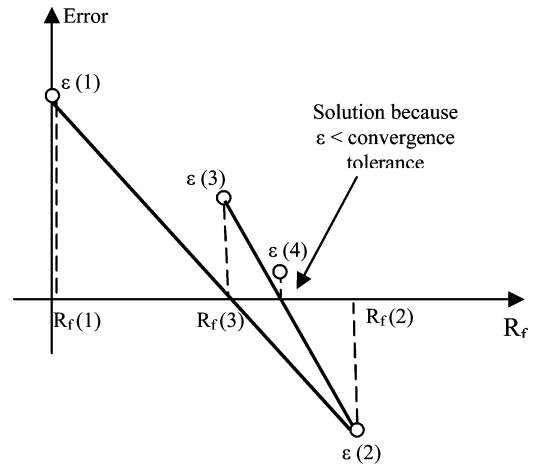
By using this voltage sag characterization method the volume of transferred data and the data that algorithm deals with is even less than transferring only the voltage sag magnitudes. In the latter, it is necessary to send magnitude of three phases in the case of three-phase faults and magnitudes of two faulted phases in the case of two-phase faults.

Reduction in the volume of recorded data by the meters is another advantage of this method. If this characterization method is not used voltage magnitudes and phase angle jumps of all phases need to be recorded. By using the characterization method only $\overline{V}$ needs to be recorded. Therefore the volume of recorded data reduces.

Moreover, computational burden of the method reduces as well. Because, instead of comparing calculated and recorded voltage angle and amplitude of three phases, only the characteristic voltages ($\overline{V}$) need to be compared. As these comparisons are carried out for the assumed fault at each node of the network, the computational burden reduces drastically.

III. ESTIMATION OF THE FAULT RESISTANCE

To estimate the fault resistance, the following procedure at each node (one at a time) should be carried out. As there is no prior knowledge about the location of the fault the following process is conducted for each node of the network, one at a time.

First, a fault with $R_f = 0$ is applied at an assumed faulted node (Start from node 1 to the last node, a node at a time). The steady state fault current at the root node (substation) is calculated using short circuit analysis method [21]. This calculated fault current is compared with the recorded current at the substation

$$\varepsilon = |I_{calculated}| - |I_{recorded}| \tag{10}$$

where $|I_{calculated}|$ is the amplitude of the calculated current phasor at the substation.

$|I_{recorded}|$ is the amplitude of the recorded current phasor at the substation.

If the amplitude of the calculated current is smaller than that of the recorded current, the assumed node cannot be the candidate location for the fault. This is because, when the fault with $R_f = 0$ at that location cannot produce the same amount of current recorded at the substation, for $R_f > 0$ it definitely cannot do so. If å does not fall within the convergence tolerance, R_f must be increased (say $R_f = 20\,\Omega$) and another iteration should be performed. By extrapolating/ interpolating the two solutions, closer estimate to the actual value of R_f is reached as shown in Fig. 3. By continuing the process, the R_f for which ε falls within the convergence tolerance can be determined.

IV. LOAD VARIATION

In order to take into account, the variation of the loads, in [9] a method has been suggested which is based on captured data at the substation. It neglects power losses in the lines, which makes it inaccurate. Here, a method based on the captured data at the substation that considers power losses in the lines is suggested. Load factor is defined as

$$L_{factor} = \frac{S_{pre-fault}}{S_{L\,\max}} \tag{11}$$

where

$$S_{L\,\max} = (M_1 + M_2 + \cdots + M_N). \tag{12}$$

N is the number of load taps and M is their nominal transformer rating.

$S_{pre-fault}$ is the pre-fault apparent power of the loads calculated at the substation, defined as follows:

$$S_{pre-fault} = |S_{substation} - S_{line}| \qquad (13)$$

where

$$S_{substation} = \sqrt{3} \times V_{Lsubstation} \times I^*_{Lsubstation} \qquad (14)$$

where $V_{Lsubstation}$ and $I_{Lsubstation}$ are the pre-fault line voltage and current at the substation calculated using a load flow program. And

$$S_{line} = U \times Z \times I^2 \times U^T \qquad (15)$$

where Z is a diagonal matrix whose diagonal elements are the impedance of each line, and I is the line currents calculated using pre-fault load flow program. U is a row-matrix whose elements are 1 and U^T is the transpose of the U matrix Now load at each tap is estimated as

$$S_i = L_{factor} * M_i. \qquad (16)$$

Knowing new S for each load, pre-fault load flow is conducted and (10), (13)–(15) are updated until S converges which means

$$|S_{Line(k)} - S_{Line(k-1)}| < \varepsilon. \qquad (17)$$

where ε is convergence tolerance and k is the iteration number.

V. Implementation of the Proposed Method

In the proposed fault location method, the characteristic voltage $(\overline{V})$ of the voltage sag, captured at some nodes along the feeder, is sent to the distribution control center. In the distribution control center, when the occurrence of the fault is detected, the pre-fault data recorded at the root node (substation) is used for updating load models. The measured during-fault characteristic voltage $(\overline{V}_{recorded})$, which was sent to the control center, and the calculated characteristic voltage $(\overline{V}_{calculated})$ obtained using short circuit analysis program are compared.

To calculate the characteristic voltage $(\overline{V}_{calculated})$ at the control center, the fault at each node is applied one at a time with the R_f values estimated using the method explained in Section III. The node at which applying the fault produces the best match between the calculated and the recorded characteristic voltages is the actual faulted node.

In some cases, when the fault occurs at those parts of the main feeder connecting the root node to the meters with R_f close to zero, all meters show almost the same voltage, which is equal to zero. In this case, phase angle of the current at root node is used to determine the location of the fault. This case will be explained in more detail in the part c of the case study section. In fact this case shows another advantage of using phase angle shift in addition to amplitude of voltage sag.

The following equation quantifies similarity between calculated and recorded voltage sag data:

$$Error = \varepsilon^2_{amplitude(V)} + \varepsilon^2_{phase(V)} + \varepsilon^2_{phase(I)} \qquad (18)$$

where $\varepsilon_{amplitude(V)}$ is the difference between the amplitude of the characteristic voltage of recorded $(\overline{V}_{recorded})$ and calculated voltage sags $(\overline{V}_{calculated})\varepsilon_{phase(V)}$ is the difference between the phase angle of the characteristic voltage of recorded $(\overline{V}_{recorded})$ and calculated voltage sags $(\overline{V}_{calculated})\varepsilon_{phase(I)}$ is the difference between the phase angle of recorded and calculated current at root node.

The following criterion is defined for faulted node detection:

$$Flag = \frac{1}{Error + \Delta} \qquad (19)$$

where Error is defined in (18) and Δ is a small number just to prevent division by zero in (19).

The node that has the largest Flag value in (19) (or smallest Error) is the faulted node. This node is one end of the faulted line (END A).

Those lines connected to END A are considered possible faulted lines. To pinpoint the fault, the fault with the R_f, calculated based on the method described in Section III, is applied at the end of these lines and moved toward END A. This trend starts from the line whose end has the largest Flag value among candidate nodes. The place in which the Flag value in (19) becomes larger than that of END A is the location of the fault. If there is no such location, it means the fault has happened at END A.

Fig. 4 shows the flowchart of the proposed algorithm. At first the measured characteristic voltage $(\overline{V}_{recorded})$ and information about the type of fault and faulted phases are provided to the method. The method presented in [22] could be used to detect type and inception of the fault. In the next step, the load models are updated as explained in Section IV. The variable "Counter" is defined to check whether the process is performed for each node of the network.

It is notable that some nodes can be easily omitted from the list of candidate nodes for fault location. For instance, those nodes that are single phase cannot be a candidate node for line-to-line faults. Step (5) checks these situations.

Moreover, as explained in Section III, if the calculated fault current with $R_f = 0$ is less than the recorded fault current at the root node, that node cannot be a candidate for fault location. Steps (6) and (7) check these cases.

Steps (8) and (9) quantify the similarity between the calculated and recorded voltage sag data. Step (10) checks whether the process has been conducted for each node of the network. One end of the faulted line (END A) is detected in step (11). Finally, the fault location is pinpointed at step (12) based on the process explained above.

VI. Case Studies

To study accuracy and performance of the proposed fault location method, the 123-node power distribution network shown in Fig. 5 is considered. This network is based on the IEEE 123-node distribution test system [23]. The network is composed of single, two, and three-phase lines with several laterals and sub-laterals, unbalanced loading with all combinations of load types (PQ, constant I, constant Z). The heterogeneity of
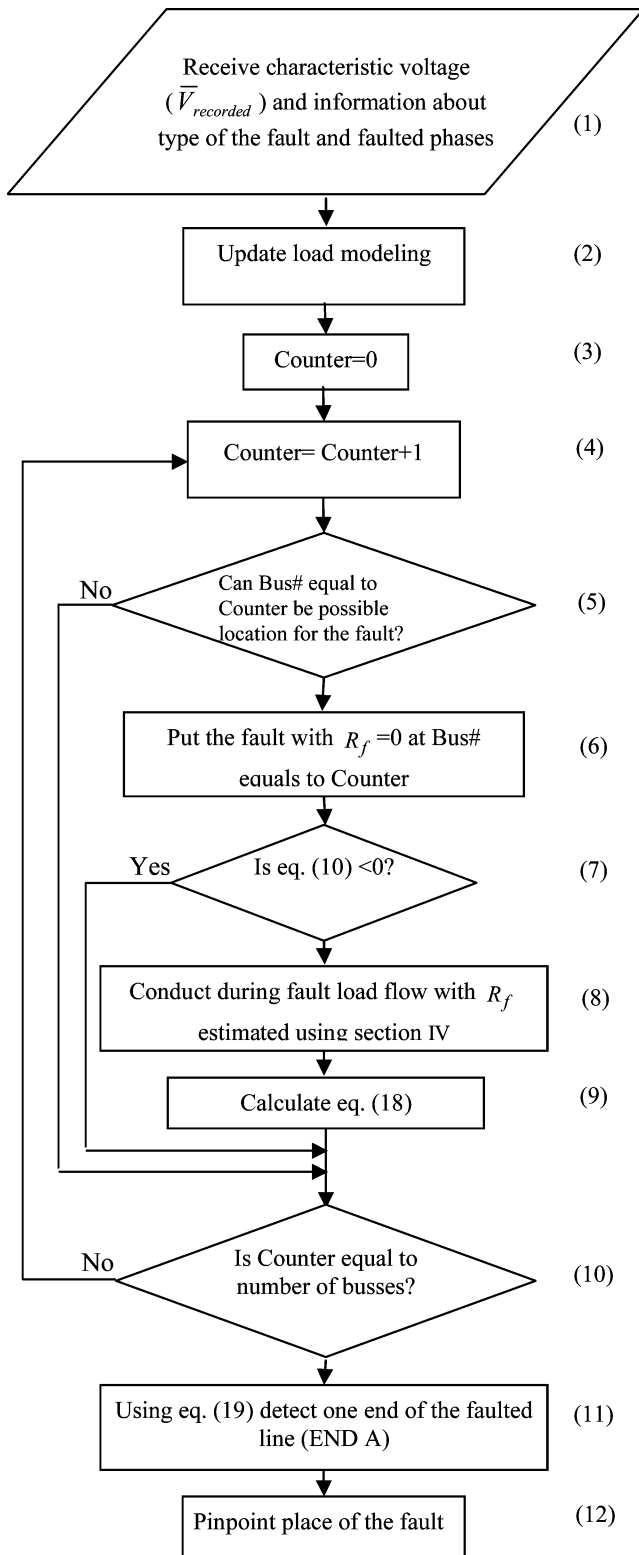
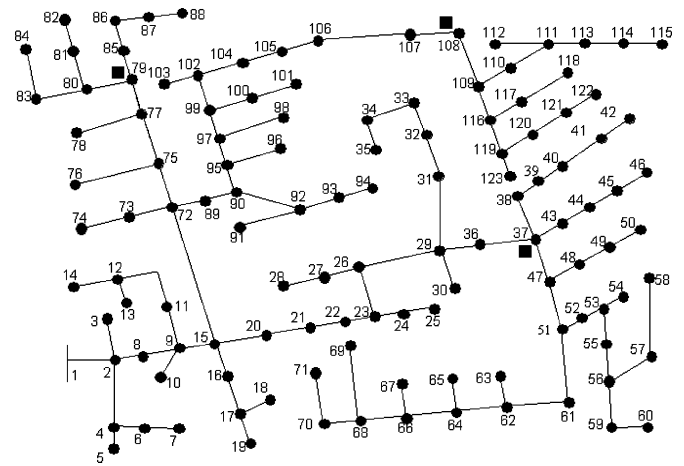Fig. 4. Flowchart of the proposed fault location algorithm.

Fig. 5. Simulated 123-node distribution system with power quality meters at nodes 37, 79, and 108.

posed in [24] that can be adopted. To take into account topology change of the network due to change in status of the switches located along the feeder, the same process should be followed for each possible configuration of the network.

The network was simulated in the ATP environment and the simulated fault data were exported to MATLAB where the full cycle Fourier filter was used to calculate the phasors.

Different fault scenarios were conducted to study the accuracy of the proposed method. Different fault types with different R_f were applied at a number of locations on the circuit.

Five cases are selected for illustration in the paper:
1) single line to ground fault (b–g) at line between node#24 and node#25;
2) line to line fault (a–c) line between node#97 and node#99;
3) three phase fault at the line between node#8 and node#9;
4) single line-ground fault (a–g) with ARC at the line between node#109 and node#116;
5) single line-ground fault (c–g) at node#29 with load variation.

The results are also compared with those of the apparent impedance-based fault location algorithm presented in [6].

A. Single Line-Ground Fault (b–g) at the Line Between Node#24 and Node#25

In this case a single line-ground fault (b–g) at line between node#24 and node#25, 10 feet or 0.0364 of the faulted line from node#24 (2210 feet from the root node) with $R_f = 1\ \Omega$ at $t = 1$ s is applied. The voltage and current at root node (node#1) as well as voltage sag data at nodes 37, 79, and 108 are captured and fault location algorithm is applied according to Fig. 4. Fig. 6 shows node#24 has the largest Flag value in (19) that means it is the actual location of the fault (END A). The possible nodes for other end are 23 and 25, which are ends of the lines connected to node#24 (END A).

Using method explained in Section V for pinpointing the fault, the fault is detected 6.2 feet or 0.0225 of the faulted line from node#24 (2206.2 feet from root node).

Comparison of the impedance-based method versus the methods proposed in this paper shows a significant difference in the resulting fault location effort. The impedance-based
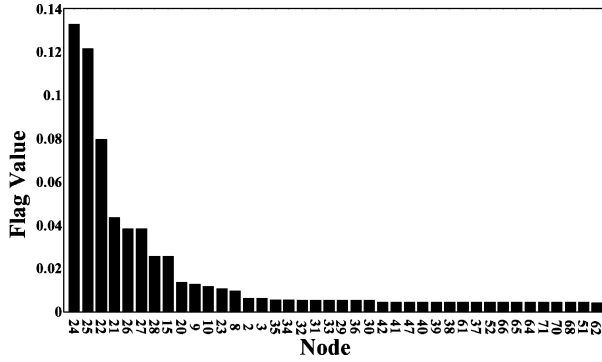
the lines is modeled by using lines with different impedance values along the feeder. It is assumed that there are three meters at nodes 37, 79, and 108 that can capture voltage sag data and send to the control center. Meters are located at nodes that capture different voltage sag levels due to faults at various locations. A systematic approach for meter placement has been pro-

Fig. 6. Flag values obtained for case A.

Fig. 8. Flag values obtained for case C.

C. Three Phase Fault at the Line Between Node#8 and Node#9

A three phase fault 80 feet or 0.4 of the faulted line from nodenode#8 (380 feet from the root node.) with $R_f = 5\ \Omega$ at $t = 0.8$ s is applied at the line between node#8 and node#9.

In this case location of the fault is mainly detected based on the phase angle shift of the current captured at the root node. Presence of the meters helps the algorithm to conclude the fault should have happened at main feeders and those parts that are common in all connection from the root node to the meters. In this way, multiple fault location estimation is prevented. Fig. 8 shows Flag values in (19) for this case.

Node#8 has the biggest Flag value that implies it is the actual location of the fault (END A). The possible nodes for other end are 2 and 9 that are ends of the lines connected to node #8 (END A). The exact place of the fault is determined to be 73.6 feet or 0.368 of the faulted line from node#8 (373.6 feet from root node).

In the case of using apparent impedance method the fault is estimated at 371.2 from the root node.

D. Single Line-Ground Fault (a–g) with ARC at the Line Between Node#109 and Node#116

In this case, a single line to ground fault that includes arc is considered at the line between node#109 and node#116, 90 feet or 0.2769 of the faulted line from node#109 (5665 feet from the root node) at $t = 1.25$ s. Arc has been modeled according to [25], [26] using MODELS language of ATP version of EMTP. The dynamic arc characteristics are simulated by the following equation:

$$\frac{dg}{dt} = \frac{1}{T}(G - g). \tag{20}$$

where T is the arc time constant, g is instantaneous arc conductance, and G is stationary arc conductance

$$G = \frac{|i_{arc}|}{u_{st}} \tag{21}$$

where

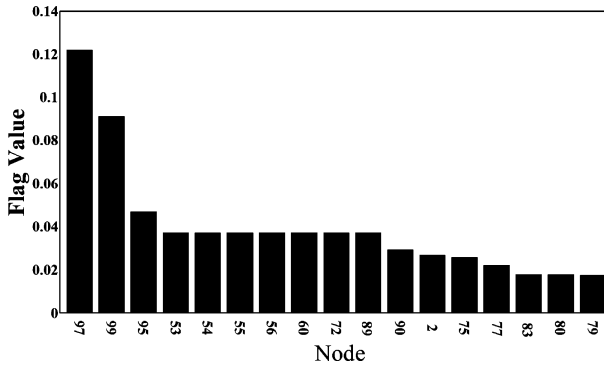$$u_{st} = u_0 + r_0 \cdot |i_{arc}|. \tag{22}$$

Fig. 7. Flag values obtained for case B.

method estimates lines between nodes 77–79, 89–90, 23–26, and 24–25 as possible locations for the fault.

To reduce the multiple fault location estimation in this network, 39 fault indicators would need to be installed at laterals and sublaterals with all data being sent to the control center. In contrast, the proposed algorithm only needs data from 3 meters for this network.

B. Line-Line Fault (a–c) at the Line Between Node#97 and Node#99

A line-line fault (a–c) at the line between node#97 and node#99, 50 feet or 0.25 of the faulted line from node#97 (2925 feet from root node) with $R_f = 10\ \Omega$ at $t = 1.1$ s is applied. Fig. 7 shows the Flag values in (19) for this case. According to the flag values, node#97 has the largest Flag that means it is the actual location of the fault (END A). The possible nodes for the other end are 95 and 99 that are ends of the lines connected to node #97 (END A). The line between nodes 97–98 cannot be the possible location for line-line fault because it only has one phase. Using the method explained in Section V for pinpointing the fault, the fault is detected 53.2 feet or 0.266 of the faulted line from node#97(2928.2 from root node).

In the case of using apparent impedance-based method, 6 places are estimated as possible locations of the fault (lines between nodes 79–80, 79–85,90–92,26–29,24–25, and 97–99)
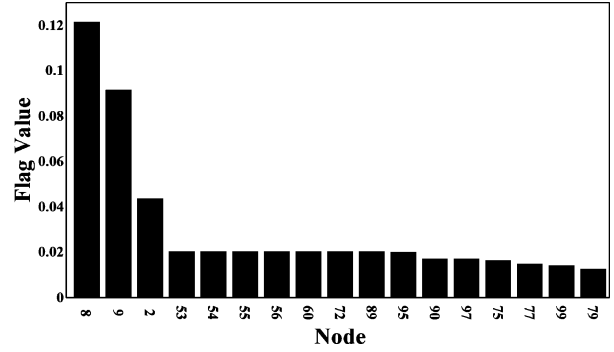
Fig. 9. Flag values obtained for case D.
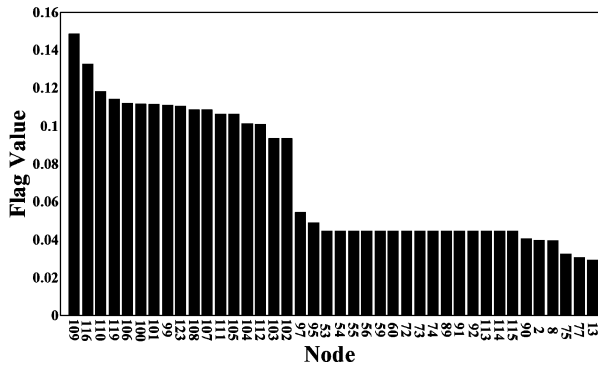

Fig. 10. Flag values obtained for case E.

i_{arc} is the instantaneous arc current, u_{st} is stationary arc voltage, u_0 is characteristic arc voltage, r_0 is characteristic arc resistance. u_0 and r_0 are defined as

$$u_0 = 0.9 \, \frac{\text{kV}}{\text{m}} \times l_{arc} + 0.4 \, \text{kV} \qquad (23)$$

$$r_0 = 40 \, \frac{\text{m}\Omega}{\text{m}} \times l_{arc} + 8 \, \text{m}\Omega \qquad (24)$$

in which l_{arc} is ARC length.

Flag values in (19) for this case are shown in Fig. 9. According to the flag values, the node #109 has the largest value that means it is the actual location of the fault (END A). The possible nodes for other end are 108, 110, and 116 that are ends of the lines connected to node #109 (END A). The location of the fault is estimated 103.7 feet or 0.3191 of the faulted line from node#109 or 5678.7 feet from the root node.

In the case of using apparent impedance method 4, places are estimated for location of the fault (lines between nodes, 59–60, 66–68, 109–110, and 109–116)

E. Single Line-Ground Fault (c–g) at Node#29 With Load Variation

In this case, the impact of load variation on the proposed fault location is studied. Load at each node is assumed as follows:

$$Load_{Actual} = Rand^* Load_{No\,min\,al} \qquad (25)$$

where rand is a random variable between zero and one. A single line-ground fault (c–g) at node#29 (or 3425 feet from the root node) with $R_f = 20 \, \Omega$ at $t = 1.13$ s is applied. Fig. 10 shows Flag values in (19) for this case. According to the flag values, the location of the fault is correctly estimated, which is node 29 that has the biggest flag value.

In the case of using apparent impedance method 3, other places are also estimated as the location of the fault (lines between nodes, 79–80, 85–86, and 97–99)

The execution time of the proposed fault location process was 37 s in the worst case and 14 s in the best case on an ordinary personal computer (PC), Processor 3 GHZ, RAM 4 GB. This shows the proposed method is very fast for practical fault location applications. Note that most of the execution time is required to run MATLAB on the PC, which is relatively slow software.
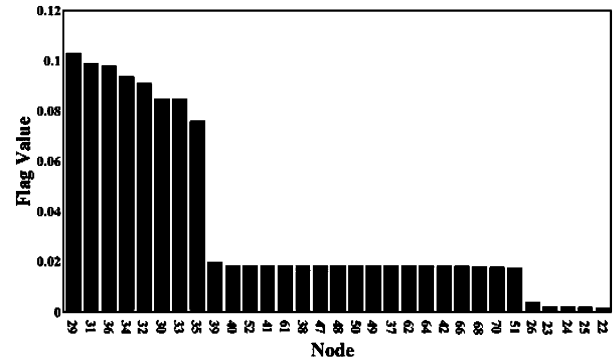
Case study results show that the proposed method can pinpoint the fault precisely. It was also shown that implementation cost of the proposed method is much less than apparent impedance-based fault location, which needs fault indicators to prevent multiple fault location estimations.

VII. CONCLUSION

In this paper, a fault location method based on voltage sag data measured at a few select locations on the distribution feeder is proposed. The accuracy of the method is demonstrated by applying different fault scenarios including arcing faults on the 123-node IEEE distribution test feeder. The demonstrated advantages of this approach are as follows.

- The algorithm provides robust results under a variety of fault scenarios.
- It can pinpoint the fault very precisely, without suffering from multiple fault location estimation imprecision, requiring high frequency sampling or retraining.
- The proposed method does not require additional analysis to decide to which estimated fault section the crew should be sent to first.
- It requires data from only a few sensors/meters located along the feeders, so its implementation cost is low.
- Since the R_f is estimated by using the proposed fast and precise approach, the R_f value does not affect the accuracy of the method.

REFERENCES

[1] R. H. Diaz and T. M. Lopez, "Fault location techniques for electrical distribution networks: A literature survey," in *Proc. 5th IASTED Int. Conf., Power and Energy Syst.*, Benalmadena, Spain, Jun. 15–17, 2005, pp. 311–318.

[2] D. Novosel, D. Hart, and J. Myllymaki, "System for locating faults and estimating fault resistance in distribution networks with tapped loads," U.S. Patent 5 839 093, 1998.

[3] A. A. Girgis, C. M. Fallon, and D. L. Lubkeman, "A fault location technique for rural distribution feeders," *IEEE Trans. Ind. Appl.*, vol. 29, no. 6, pp. 1170–1175, Dec. 1993.

[4] K. Srinivasan and A. St-Jacques, "A new fault location algorithm for radial transmission lines with loads," *IEEE Trans. Power Del.*, vol. 18, no. 3, pp. 1679–1682, Jul. 2003.

[5] J. Mora-Florez, J. Melendez, and G. Carrillo-Caicedo, "Comparison of impedance fault location methods for power distribution systems," *Elect. Power Syst. Res.*, vol. 78, pp. 657–666, 2008.

[6] R. Das, "Determining the locations of faults in distribution systems," Ph.D. dissertation, Elect. Eng. Dept., Saskatchewan Univ., Saskatoon, SK, Canada, 1998.

[7] M. S. Choi, S. J. Lee, D. S. Lee, and B. G. Jin, "A new fault location algorithm using direct circuit analysis for distribution systems," *IEEE Trans. Power Del.*, vol. 19, no. 1, pp. 35–41, Jan. 2004.

[8] M. S. Choi, S. J. Lee, S. I. Lim, D. S. Lee, and X. Yang, "A direct three-phase circuit analysis- fault location for line-to-line fault," *IEEE Trans. Power Del*, vol. 22, no. 4, pp. 2541–2547, Oct. 2007.

[9] R. K. Aggarwal, Y. Aslan, and A. T. Johns, "New concept in fault location for overhead distribution systems using superimposed components," *Proc. Inst. Elect. Eng., Gen., Transm., Distrib.*, vol. 144, no. 3, pp. 309–316, May 1997.

[10] R. K. Aggarwal, Y. Aslan, and A. T. Johns, "An interactive approach to fault location on overhead distribution lines with load taps," in *Developments in Power System Protection*, Mar. 25–27, 1997, pp. 184–187.

[11] J. J. Mora, G. Carrillo, and L. Perez, "Fault location in power distribution systems using ANFIS nets and current patterns," in *Proc. IEEE Power Eng. Soc. Transmission and Distribution Conf. Expo. Latin America*, Venezuela, 2006, pp. 1–7.

[12] J. Mora-Florez, V. Barrera-Nuez, and G. Carrillo-Caicedo, "Fault location inower distribution systems using a learning algorithm for multivariable data analysis," *IEEE Trans. Power Del.*, vol. 22, no. 3, pp. 1715–1721, Jul. 2007.

[13] Z. Q. Bo, G. Weller, and M. A. Redfern, "Accurate fault location technique for distribution system using fault-generated high-frequency transient voltage signals," *Proc. Inst. Elect. Eng., Gen. Transm. Distrib.*, vol. 146, no. 1, Jan. 1999.

[14] D. W. P. Thomas, R. J. O. Carvalho, and E. T. Pereira, "Fault location in distribution systems on traveling waves," presented at the IEEE Bologna Power Tech Conf., Bologna, Italy, Jun. 23–26, 2003.

[15] H. Nouri, C. Wang, and T. Davies, "An accurate fault location technique for distribution lines with tapped loads using wavelet transform," in *Proc. IEEE Power Tech*, Porto, Portugal, Sep. 10–13, 2001, vol. 3, pp. 1–4.

[16] T. A. Short, D. D. Sabin, and M. F. McGranaghan, "Using PQ monitoring and substation relays for fault location on distribution systems," in *Proc. IEEE Rural Electric Power Conf.*, May 6–7, 2007, pp. B4-1–B4-7.

[17] R. A. F. Pereira, L. G. W. Silva, M. Kezunovic, and J. R. S. Mantovani, "Improved fault location on distribution feeders on matching during-fault voltage sags," *IEEE Trans. Power Del.*, vol. 24, no. 2, pp. 852–862, Apr. 2009.

[18] Z. Galijasevic and A. Abur, "Fault location using voltage measurements," *IEEE Trans. Power Del*, vol. 17, no. 2, pp. 441–445, Apr. 2002.

[19] M. H. J. Bollen, *Understanding Power Quality Problems: Voltage Sags and Interruptions*. New York: IEEE, 1999.

[20] M. H. J. Bollen, "Algorithm for characterizing measured three-phase unbalanced voltage dips," *IEEE Trans. Power Del.*, vol. 18, no. 3, pp. 937–944, Jul. 2003.

[21] Y. Mao and K. N. Miu, "Radial distribution system short circuit analysis with lateral and load equivalencing: Solution algorithms and numerical results," in *Proc. IEEE Power Eng. Soc. Summer Meeting*, 2000, vol. 1, pp. 449–453.

[22] M. Kezunovic, P. Spasojevic, C. Fromen, and D. Sevcik, "An expert system for transmission substation event analysis," *IEEE Trans. Power Del.*, vol. 8, no. 4, pp. 1942–1949, Oct. 1993.

[23] Radial distribution test feeders. Distribution System Analysis Subcommittee Rep. [Online]. Available: http://ewh.ieee.org/soc/pes/dsacom/testfeeders.html

[24] R. A. F. Pereira, L. G. W. da Silva, and J. R. S. Mantovani, "PMUs optimized allocation using a tabu search algorithm for fault location in electric power distribution system," presented at the Latin America Transmission and Distribution Conf. Expo. Sao Paulo, Brazil, 2004.

[25] M. Kizilcay and K. H. Koch, "Numerical fault arc simulation on power arc tests," *Eur. Trans. Elect. Power*, vol. 4, no. 3, pp. 177–186, May/Jun. 1994.

[26] M. Kizilcay and P. L. Seta, "Digital simulation of fault arcs in medium-voltage distribution networks," in *Proc. 15th PSCC*, Liege, Belgium, Aug. 22–26, 2005, pp. 1–7.

Saeed Lotfifard (S'08) is currently pursuing the Ph.D. degree at Texas A&M University, College Station.

His research interests are power systems protection and control, intelligent monitoring and outage management-self healing grids, distribution automation, cyber-physical energy system/smart grid technologies, and applications of statistical methods and signal processing in power systems.

Mladen Kezunovic (S'77–M'80–SM'85–F'99) received the Dipl.Ing. degree from the University of Sarajevo in 1974, and the M.S. and Ph.D. degrees in electrical engineering from the University of Kansas in 1977 and 1980, respectively.

Currently, he is the Eugene E. Webb Professor and Site Director of the Power Engineering Research Center (PSerc), an NSF I/UCRC at Texas A&M University, College Station. He was with Westinghouse Electric Corp., Pittsburgh, PA, from 1979 to 1980 and the Energoinvest Co. in Europe from 1980 to 1986, and spent a sabbatical at EdF in Clamart, France, from 1999 to 2000. He was also a Visiting Professor at Washington State University, Pullman, from 1986 to 1987 and The University of Hong Kong in 2007. His main research interests are digital simulators and simulation methods for relay testing as well as the application of intelligent methods to power system monitoring, control, and protection.

Dr. Kezunovic is a member of CIGRE and a Registered Professional Engineer in Texas.

Mirrasoul J. Mousavi (S'01–M'05) received the Ph.D. degree in electrical engineering from Texas A&M University, College Station.

Currently, he is with the ABB US Corporate Research Center, responsible for leading projects related to power system automation, monitoring, and diagnostics. He was a Researcher in the Power System Automation Laboratory and a Graduate Lecturer at Texas A&M University prior to joining ABB. From 1999 to 2001, he was involved in R&D with Niroo Research Institute (NRI). His current professional interests are related to power system automation, fault diagnosis, asset management, as well as power system modeling and simulation.

Dr. Mousavi is a member of the IEEE Power and Energy Society and IEEE Dielectrics and Electrical Insulation Society.